

A Young Planetary-Mass Object in the ρ Oph Cloud Core

Kenneth A. Marsh, J. Davy Kirkpatrick and Peter Plavchan

Infrared Processing and Analysis Center, California Institute of Technology 100-22,
Pasadena, CA 91125;

kam@ipac.caltech.edu, davy@ipac.caltech.edu, plavchan@ipac.caltech.edu

Received _____; accepted _____

To be published in ApJ Letters

ABSTRACT

We report the discovery of a young planetary-mass brown dwarf in the ρ Oph cloud core. The object was identified as such with the aid of a 1.5–2.4 μm low-resolution spectrum obtained using the NIRC instrument on the Keck I telescope. Based on the COND model, the observed spectrum is consistent with a reddened ($A_V \sim 15 - 16$) brown dwarf whose effective temperature is in the range 1200–1800 K. For an assumed age of 1 Myr, comparison with isochrones further constrains the temperature to ~ 1400 K and suggests a mass of $\sim 2-3$ Jupiter masses. The inferred temperature is suggestive of an early T spectral type, which is supported by spectral morphology consistent with weak methane absorption. Based on its inferred distance (~ 100 pc) and the presence of overlying visual absorption, it is very likely to be a ρ Oph cluster member. In addition, given the estimated spectral type, it may be the youngest and least massive T dwarf found so far. Its existence suggests that the initial mass function for the ρ Oph star-forming region extends well into the planetary-mass regime.

Subject headings: stars: low-mass, brown dwarfs — stars: pre-main sequence —
infrared: stars

1. Introduction

Free-floating planetary-mass objects have been purported in young clusters such as σ Orionis (Zapatero Osorio et al. 2002) and the Trapezium (Lucas et al. 2006). These are brown dwarfs whose masses are below the deuterium-burning limit of 13 Jupiter masses (M_{Jup}), and their existence imposes severe restrictions on brown dwarf formation models. The models must account both for the generation of low-mass cloud fragments and also for their subsequent collapse. In principle, the required masses can be produced by mechanisms such as fragmentation of collapsing protostellar cores (Boss 2001) or encounters between protostellar disks (Shen & Wadsley 2006), but this still leaves the problem of providing the necessary cooling to allow gravity to overcome gas pressure. In this regard, recent work by Whitworth & Stamatellos (2006) suggests that masses as low as 1-4 M_{Jup} are possible, the lower limit being independent of the particular star formation scenario. However, difficulties still arise when subsequent accretion is taken into account, since this can greatly increase the final mass of the object. Subsequent dynamical ejection may be necessary in order to prevent this mass gain (see, for example, Reipurth & Clarke (2001)). A key constraint on these models could be provided by observational determination of the form of the initial mass function, and, in particular, whether there is a minimum mass for brown dwarf formation. The latter would provide a key test of the prediction of Whitworth & Stamatellos (2006), even though additional tests would be required in order to distinguish between the possible fragmentation mechanisms.

With this in mind, we have begun a spectroscopic study of objects in the ρ Oph cloud core whose near-infrared colors are suggestive of low-mass brown dwarfs. This region is a particularly suitable site for the study of young brown dwarfs due to its youth, high rate of low-mass star formation and its relative proximity at a distance of ~ 120 – 130 pc (Loinard et al. 2008; Mamajek 2008; Lombardi et al. 2008). We have produced a list of

brown dwarf candidates in a $1^\circ \times 9'$ region of the cloud core, based on deep integration J , H , and K_s images from the stacked calibration scans of 2MASS (Cutri et al. 2006) together with *Spitzer* IRAC images at 3.6, 4.5, 5.8 and 8.0 μm . Our selection technique is based on the estimated effective temperature, obtained from fits of the observed spectral energy distributions (SEDs) to atmospheric models (Marsh et al., in preparation). In a pilot program of spectroscopic observations, we have observed seven candidates from this list using the NIRC instrument on the Keck I telescope, and now present the results. In particular, we report the first discovery of a planetary-mass brown dwarf in ρ Oph.

2. Observations and Data Reduction

We selected seven brown dwarf candidates whose near-infrared colors suggested effective temperatures less than 2000 K. These objects are listed in Table 1; each is labeled with an ID number based on the ordering of our source extractions in the $1^\circ \times 9'$ 2MASS Deep Field; the full list will be presented in the near future by Marsh et al. We observed these objects using the NIRC instrument (Matthews & Soiffer 1994) on the 10-m Keck I telescope on the night of 2009 May 27 (UT). NIRC was used in grism mode (grism gr120), with a slit width of 3.5 pixels, to produce low-resolution ($R \sim 90$) spectra in the wavelength range 1.5–2.4 μm . Conditions were essentially clear except for light cirrus haze, and the seeing was $\sim 0.6''$.

Targets were located on the slit by first imaging them in the K -band continuum. They were then observed in grism mode in sets of 30 s or 60 s exposures, using a nodding pattern in which the telescope was dithered at intervals of $5''$ along the slit. Typically, 5 such sets were coadded.

The coadded images were pair-wise subtracted to remove the dark current and sky

background, and divided by a flat-field image to remove pixel-to-pixel gain variations. The latter image was derived from observations of the telescope dome after subtraction of the dark response. It was also used in the construction of a bad pixel mask. Correction for the spectral response of the instrument and absorption by the telluric bands of the atmosphere was then obtained from observations of A0 stars Oph S1 and HD 161743. The correction was applied by multiplying the spectrum of a program star by a 10,000 K black body spectrum and dividing by the observed spectrum of the A0 star. In doing so, it was necessary to deredden the Oph S1 spectrum to correct for the known 10 magnitudes of visual absorption (Gagné et al. 2004). For telluric correction we also utilized an observation of NGC 4361, a planetary nebula whose HK spectrum is dominated by the continuum of the hot central star. Wavelength calibration was accomplished using a cubic fit to a set of atmospheric OH lines identified in sky observations based on Rousselot et al. (2000), and a set of nebular lines from an observation of another planetary nebula, G049.3+88.1.

The maximum likelihood estimate of the spectrum of each program object was obtained using all available observations for that object simultaneously. This necessitated spatial co-registration of the individual subtracted nods, accomplished by adjusting the image offset parallel to the slit based on maximum correlation of the signal with the wavelength-dependent spatial point spread function (PSF). The latter was estimated using observations of strong calibrators. The program star spectrum was then obtained from a series of maximum likelihood flux estimates as a function of wavelength using all observations which fell within a rectangular “fitting” window of width typically 9 pixels in both the spatial and spectral directions, where 1 pixel corresponds to $0.15''$ and $\sim 0.005 \mu\text{m}$, respectively; the spectral boxcar width was, however, increased to 21 pixels for #4450, the object with lowest S/N . The estimation procedure involved knowledge of the measurement noise, estimated from adjacent strips on the image, external to the strip containing the signal. In order to minimize the effect of spikes due to cosmic ray hits, it was necessary

to use trimmed averaging during noise estimation, and 3σ outlier rejection during spectral estimation. The estimated spectra of our seven program objects are shown by the solid lines in Figures 1 and 2. Also included in Figure 2, for comparison, are our spectra of two known T dwarfs, SDSS 1254-0122 (T2) and 2MASS 1503+2525 (T5.5).

3. Model Fitting

The observations have been fitted to a grid of synthetic spectra based on photospheric models described by Allard et al. (2001, 2003) and Hauschildt et al. (1999), and downloaded from the Lyon group’s website¹. The grid covers the range $T_{\text{eff}} = 100\text{--}10,000$ K in effective temperature and $\log g = 2.5\text{--}6.0$ cm s⁻² in surface gravity; we have assumed solar metallicity. The temperature range is spanned by four models (COND, SETTL, DUSTY and NextGen), each of which covers a particular regime with respect to dust grain formation; the COND model is applicable to methane dwarfs ($T \lesssim 1500$ K).

For each of these models we have calculated the inverse-variance weighted sum of squares of residuals between the model (smoothed to the resolution of the observations) and the observed spectrum of a given object. During this procedure it was necessary to redden the model spectra since objects in the ρ Oph cloud are seen through a substantial amount of extinction; for this purpose the Cardelli et al. (1989) reddening law was used. For each object, the unknowns were therefore: T_{eff} , $\log g$, A_V , and the model type. Maximum likelihood estimates of these parameters were obtained by minimizing the mean square residual over the wavelength range 1.5–2.4 μm (excluding 1.7–2.0 μm to avoid the deep telluric absorption bands), and the results are presented in the last four columns of Table 1. The corresponding model spectra are plotted as dashed lines in Figures 1 and 2.

¹<http://phoenix.ens-lyon.fr/Grids>

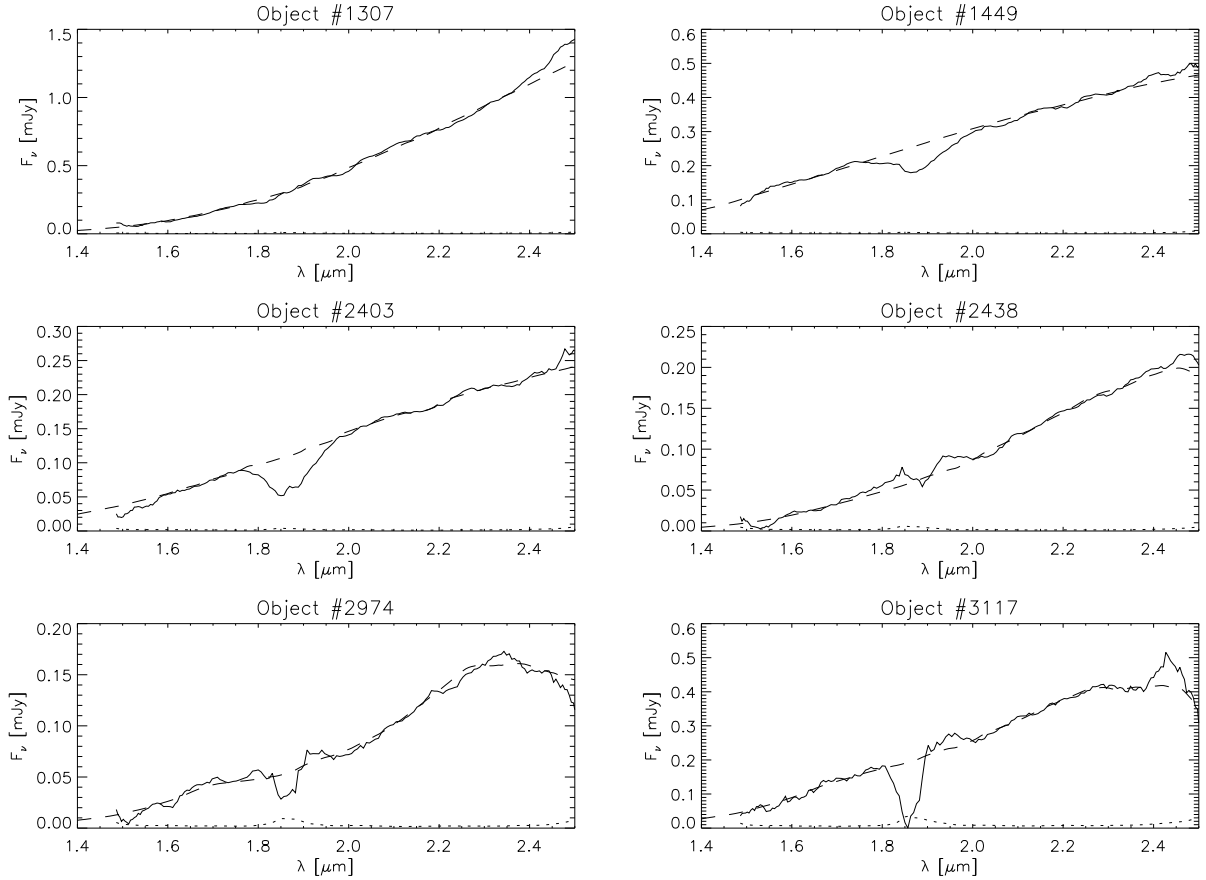


Fig. 1.— Spectra of six of the seven candidate objects. In each case, the solid line represents the observed spectrum and the dotted line represents the uncertainty due to uncorrelated measurement noise; the dashed line represents the best-fit model spectrum. A boxcar averaging window of width 9 pixels ($0.045 \mu\text{m}$) has been applied in all cases. Peak S/N values for the six spectra (after smoothing), in order of object ID number, are: 248, 192, 156, 126, 87, and 57. Note that the pronounced dips at $\sim 1.85 \mu\text{m}$ represent an artifact due to imperfect correction for the deep telluric absorption bands.

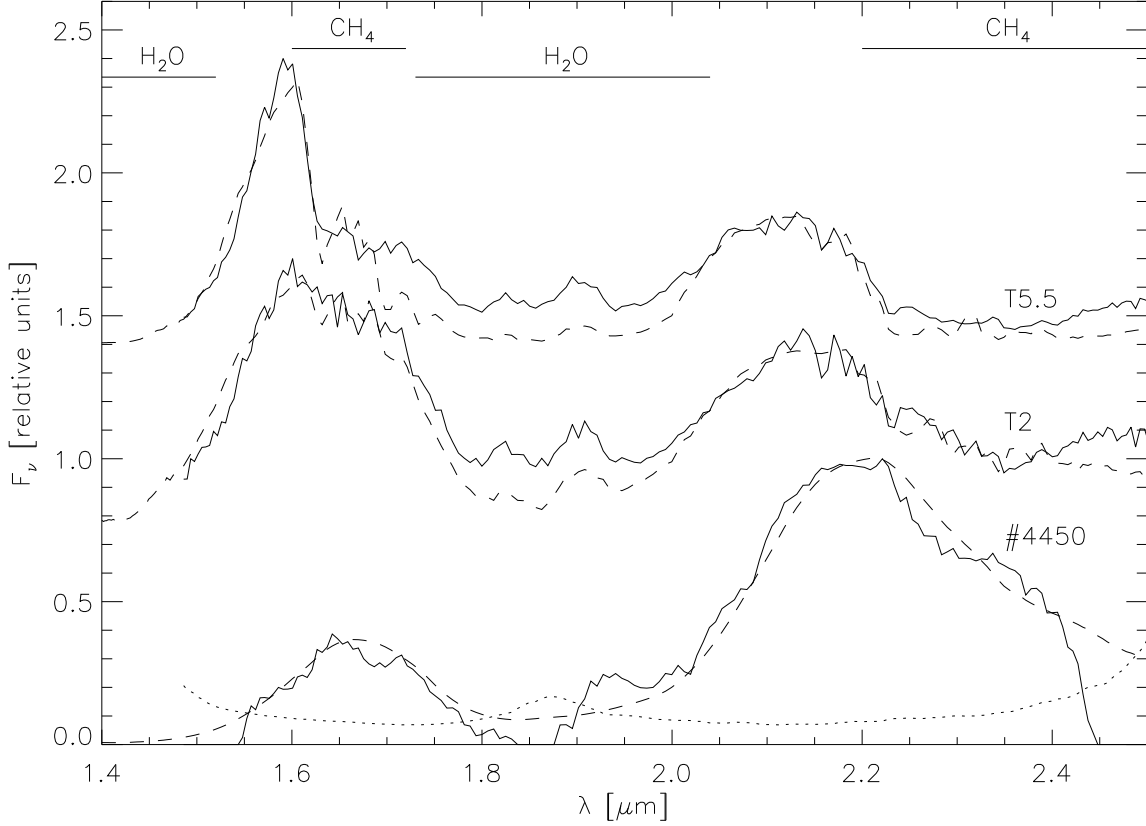


Fig. 2.— Spectra of object #4450 and the two known T dwarfs, SDSS 1254-0122 (T2) and 2MASS 1503+2525 (T5.5), normalized to peak fluxes of 0.075, 3.6, and 6.2 mJy, respectively. For clarity, the T2 and T5.5 spectra have been displaced vertically by 0.7 and 1.4 units, respectively. In each case, the solid line represents the observed spectrum and the dashed line represents the best-fit model spectrum. The dotted line represents the RMS measurement noise in the #4450 spectrum. A boxcar averaging window of width 21 pixels ($0.1 \mu\text{m}$) was used in the estimation of the #4450 spectrum, but no averaging was used for the other two objects. The peak SNR of the smoothed #4450 spectrum was 13.5; the peak SNRs for SDS 1254-0122 and 2MASS 1503+2525 were 1188 and 1848, respectively. The approximate extents of the water and methane absorption bands are indicated at the top.

One of the objects (#4450) has a spectrum which resembles a reddened version of SDSS 1254-0122 (T2), and the model fitting results confirm its identity as a moderately cool brown dwarf. The spectrum is suggestive of a low gravity object, as evidenced by the steeper falloff on the short wavelength side of the H -band peak with respect to that of the field dwarfs in Figure 2, and the displacement of the K -band peak to a longer wavelength—both of these features are consistent with the much deeper H_2O absorption expected in a lower gravity object.

The maximum likelihood parameter estimates based on the observed NIRC spectrum are: $T_{\text{eff}} = 1600_{-450}^{+250}$ K, $\log g = 4.5_{-2.0}^{+0.8}$ and $A_V = 24.5$ with an uncertainty of $\sim \pm 10$ mag. The large uncertainty in A_V is due to the relatively low S/N which allows for a fairly large range in model temperatures. To gain more leverage for the A_V estimate and to further constrain the other parameters, we repeated the model fitting incorporating the IRAC [3.6] and [4.5] magnitudes (15.77 ± 0.13 and 15.85 ± 0.10 , respectively; Marsh et al., in preparation). We obtained: $T_{\text{eff}} = 1400 \pm 100$ K, $\log g = 3.0_{-0.5}^{+1.7}$, $A_V = 15.6 \pm 2.5$; the corresponding fit to the dereddened spectrum (+ IRAC fluxes) is shown in Figure 3.

4. Discussion

The results of model fitting indicate that:

1. The estimated temperatures for the two known T dwarfs are consistent with the previously-published spectral types (Burgasser et al. 2003; Dahn et al. 2002). They also indicate surface gravities characteristic of mature brown dwarfs, and zero visual absorption within the error bars, as expected. These two results have therefore provided a useful check on our observing and data reduction techniques. This is particularly significant in view of Burgasser et al. (2004)’s finding that model fits to

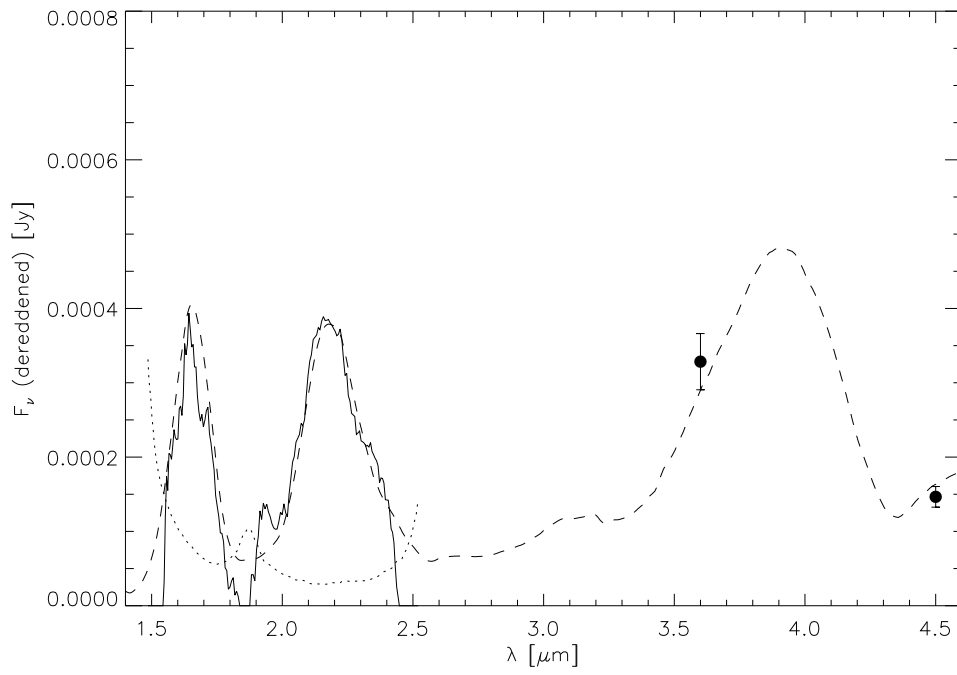


Fig. 3.— De-reddened spectrum of object #4450 (solid line), and the best-fit model (dashed line) based on $T_{\text{eff}} = 1400$ K and $\log g = 3.0$. The dotted line represents the uncertainty in the observed spectrum and the filled circles represent the IRAC fluxes at 3.6 and 4.5 μm .

some T dwarf spectra yield anomalously low surface gravities. However that bias occurred only for late T dwarfs (T7 onwards), and hence there is no disagreement with the present results.

2. For all except object #4450, the spectroscopically-estimated temperature is substantially higher than the $T_{\text{eff}} < 2000$ K values inferred from our previous SED fits. These other six objects are most likely T Tau stars and/or reddened background stars. One possible exception is #2974, whose error bars place it within reach of being a brown dwarf near the hydrogen-burning limit (its observed spectrum is consistent with $T_{\text{eff}} = 2800$ K & $\log g = 4.0$, corresponding to a mass as low as $0.05 M_{\odot}$ based on the isochrones of Baraffe et al. (2003)). In our forthcoming paper (Marsh et al., in preparation) we discuss the likely reason for the six underestimated temperatures, and have used the results to improve our SED fitting procedure.
3. Object #4450 is a low-gravity brown dwarf whose estimated temperature suggests an early T spectral type. This is supported by the presence of weak, broad absorption features on the long wavelength sides of the H and K peaks (see Figure 2), suggestive of methane. Definitive identification of methane will, however, need to await future observations at higher spectral resolution and signal to noise ratio.

Figure 4 shows the estimated location of #4450 in the $\log g$ - T_{eff} plane, together with the 1σ contour of the model fitting solution. Also superposed on the figure is a set of isochrones for the COND model, from Baraffe et al. (2003). If we take the estimated age of 1 Myr for the ρ Oph cloud (Luhman & Rieke 1999; Prato et al. 2003; Wilking et al. 2005), the isochrones further constrain the parameters of this object. Specifically, the intersection of the 1σ contour and the 1 Myr isochrone corresponds to $T_{\text{eff}} \sim 1400$ K and $\log g \sim 3.3$; such a temperature reinforces our estimate of early T spectral type. The corresponding mass would be $\sim 2 - 3 M_{\text{Jup}}$, making #4450 a candidate for the lowest-mass object outside

our solar system to have been imaged to date. Another candidate for this distinction is S Ori 70 (Zapatero Osorio et al. 2002; Martin & Zapatero Osorio 2003), whose parameters are also indicated on Figure 4. We note, however, that the identification of S Ori 70 as a young, low-gravity member of the σ Orionis cluster has been called into question by Burgasser et al. (2004), who find that the observed spectra of that object could equally well be interpreted in terms of an old field T dwarf of much higher mass.

We can estimate a distance to #4450 by comparing the apparent and absolute magnitudes, obtained from the observations and model, respectively. If we assume an age of 1 Myr, then the corresponding isochrone in Figure 4 indicates a range 1360–1610 K of T_{eff} values from the spectral fits; the corresponding range in M_K , obtained by spline interpolation of the isochronal values from Baraffe et al. (2003), is then 11.64–10.72. Comparison with the dereddened apparent K magnitude of 15.86 ± 0.23 , assuming that all of the uncertainties add in quadrature, then leads to a $\pm 1\sigma$ range in distance of 68–111 pc. Although this might suggest that #4450 is closer than ρ Oph, based on most distance estimates (120–130 pc), this range is in fact, consistent with the recent 119 ± 6 pc estimate of Lombardi et al. (2008) when account is taken of the finite thickness of the cloud along the line of sight (28_{-19}^{+29} pc). Our results are therefore consistent with #4450 being located near the front edge of the ρ Oph cloud. If the object is older than 1 Myr, the estimated distance decreases, since older objects are less bloated and therefore must be closer to maintain the same flux. If, for example, we assume an age of 100 Myr (the largest age within the 1σ contour of Figure 4), the distance upper limit gets reduced to ~ 86 pc.

What evidence do we have that object #4450 is a ρ Oph cluster member and not simply a foreground or background T dwarf? We can readily exclude the former possibility because of the presence of substantial visual extinction. Also, an old background T dwarf is excluded since it would have insufficient flux, based on the discussion in the previous

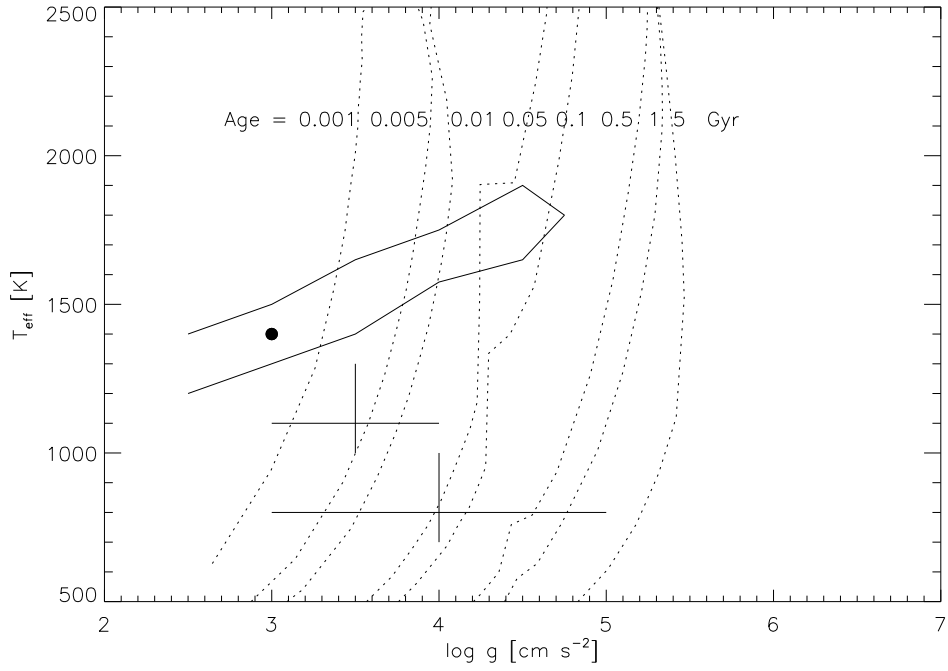


Fig. 4.— Results of model fitting for object #4450, in the $\log g$ – T_{eff} plane. The best fit to the observed spectrum is indicated by the filled circle, and the 1σ uncertainty is indicated by the solid contour. The dotted lines represent isochrones from Baraffe et al. (2003). For comparison, the crosses represent the estimated parameters of S Ori 70, another arguably young object of comparable mass (Zapatero Osorio et al. 2002; Martin & Zapatero Osorio 2003).

paragraph. However, since the line of sight to #4450 intersects the southeastern portion of the Upper Sco association (de Zeeuw et al. 1999), we must consider the latter as another possible location, which would imply an age of ~ 5 Myr (Mamajek 2008). However, the 145 pc distance of Upper Sco (Mamajek 2008) is almost 3σ beyond the estimated distance of #4450 and hence membership in ρ Oph is much more likely. In either case, the estimated mass would still be $\lesssim 3 M_{\text{Jup}}$.

Our conclusions regarding the nature of this object could be tested by future observations at higher spectral resolution (~ 1000), with an instrument such as NIRSPEC (McLean et al. 1998), particularly if the wavelength range were extended to include the J -band. Measurement of key flux ratios of H_2O and CH_4 features (see McLean et al. (2003)) would then facilitate more accurate spectral typing, and the gravity estimate could be refined using the K I doublet lines near $1.25 \mu\text{m}$. Comparison of the resulting T_{eff} and $\log g$ with the COND isochrones might then lead to a better constraint on the age which, in the present analysis, has been assumed to be 1 Myr based on sky location in the ρ Oph cloud.

Our detection of this object suggests that the initial mass function for the ρ Oph star-forming region extends well into the planetary-mass regime. Object #4450 is, however, only one of about a dozen objects within our $1^\circ \times 9'$ region of study whose near-infrared SEDs are similarly indicative of planetary-mass brown dwarfs, and we plan to obtain near infrared spectra of these objects in the near future. We thereby hope to accumulate some statistics on the low end of the brown dwarf mass function to further our goal of constraining the formation models. In this regard, we also look forward to the expected wealth of information from the Wide-field Infrared Survey Explorer (WISE) mission, which will provide an inventory of low-mass cold brown dwarfs in the immediate solar neighborhood.

We thank the referee (A. Muench) for helpful comments. The data presented herein were obtained at the W.M. Keck Observatory, which is operated as a scientific partnership among the California Institute of Technology, the University of California and the National Aeronautics and Space Administration. The Observatory was made possible by the generous financial support of the W.M. Keck Foundation. The authors wish to recognize and acknowledge the very significant cultural role and reverence that the summit of Mauna Kea has always had within the indigenous Hawaiian community. We are most fortunate to have the opportunity to conduct observations from this mountain. Our research also utilized the Simbad database, operated at CDS, Strasbourg, France. The work was carried out at IPAC/Caltech and was supported by a grant from the NASA Astrophysics Data Analysis Program and by a Keck PI data award.

REFERENCES

- Allard, F., Hauschildt, P. H., Alexander, D. R., Tamanai, A. & Schweitzer, A. 2001, *ApJ*, 556, 357
- Allard, F., Guillot, T., Ludwig, H.-G., Hauschildt, P. H., Alexander, D. R. & Schweitzer, A. 2003, in *Brown Dwarfs*, ed. E. Martin (San Francisco: ASP), IAU Symp., 211, 325
- Baraffe, I., Chabrier, G., Barman, T. S., Allard, F. & Hauschildt, P. H. 2003, *A&A*, 402, 701
- Boss, A. 2001, *ApJ*, 551, 167
- Burgasser, A. J., Kirkpatrick, J. D., McElwain, M. W., Cutri, R. M., Burgasser, A. J., & Skrutskie, M. F. 2003, *AJ*, 125, 850
- Burgasser, A. J., Kirkpatrick, J. D., McGovern, M. R., McLean, I. S., Prato, L. & Reid, I. N. 2004, *ApJ*, 604, 827
- Cardelli, J., Clayton, G. & Mathis, J. 1989, *ApJ*, 345, 245
- Cutri, R. et al. 2006, Explanatory Supplement to the 2MASS All Sky Data Release and Extended Mission Products, <http://www.ipac.caltech.edu/2mass/releases/allsky/doc/explsup.html>.
- Dahn, C. C. et al. 2002, *AJ*, 124, 1170
- de Zeeuw, P. T., Hoogerwerf, R., de Bruijne, J. H. J., Brown, A. G. A., & Blaauw, A. 1999, *AJ*, 117, 354
- Gagné, M., Skinner, S. L. & Daniel, K. J. 2004, *ApJ*, 613, 393
- Hauschildt, P. H., Allard, F. & Baron, E. 1999, *ApJ*, 512, 377

- Leggett, S. K. et al. 2000, *ApJ*, 536, L35
- Loinard, L., Torres, R. M., Mioduszewski, A. & Rodriguez, L. F. 2008, *ApJ*, 675, L29
- Lombardi, M., Lada, C. J., & Alves, J. 2008, *A&A*, 489, 143
- Lucas, P. W., Weights, D. J., Roche, P. F. & Riddick, F. C. 2006, *MNRAS*, 373, 60
- Luhman, K. L. & Rieke, G. H. 1999, *ApJ*, 525, 440
- Mamajek, E. E. 2008, *AN*, 329, 10
- Martin, E. L. & Zapatero Osorio, M. R. 2003, *ApJ*, 593, L113
- Matthews, K. & Soifer, B. T. 1994, *Exp. Astron.*, 3, 77
- McLean, I. S. et al. 1998, *SPIE*, 3354, 566
- McLean, I. S., McGovern, M. R., Burgasser, A. J., Kirkpatrick, J. D., Prato, L. & Kim, S. S. 2003, *ApJ*, 596, 561
- Prato, L., Greene, T. P. & Simon, M. 2003, *ApJ*, 584, 853
- Reipurth, B. & Clarke, C. 2001, *AJ*, 122, 432
- Rousselot, P., Lidman, C., Cuby, J.-G., Moreels, G. & Monnet, G. 2000, *A&A*, 354, 1134
- Shen, S. & Wadsley, J. 2006, *ApJ*, 651, L145
- Whitworth, A. P. & Stamatellos, D. 2006, *A&A*, 458, 817
- Wiling, B. A., Meyer, M. R., Robinson, J. G. & Greene, T. P. 2005, *AJ*, 130, 1733
- Zapatero Osorio, M. R., Béjar, V. J. S., Martín, E. L., Rebolo, R., Barrado y Navascués, D., Mundt, R., Eislöffel, J. & Caballero, J. A. 2002, *ApJ*, 578, 536

Table 1. Observational and model-fitted parameters.

Object ID	Type ^a	RA	Dec	K	$t_{\text{int}}^{\text{b}}$ [s]	A.M. ^c	T_{eff} [K]	$\log g^{\text{d}}$ [cm s ⁻²]	A_V^{e} [mag]	Mod. ^f
#1307 ^g	bdc	16 27 32.89	-24 28 11.4	14.92	360	1.68	> 4800	indet.	36.1	N
#1449	bdc	16 27 30.36	-24 20 52.2	15.67	900	1.40	> 5700	indet.	21.4	N
#2403	bdc	16 27 21.63	-24 32 19.2	16.42	900	1.70	> 5200	indet.	24.5	N
#2438	bdc	16 27 09.37	-24 32 14.9	16.74	900	1.92	> 3500	indet.	32.7	D
#2974	bdc	16 27 16.74	-24 25 39.0	16.86	900	2.20	3200 ⁺³⁰⁰ ₋₄₀₀	indet.	25.9	D
#3117	bdc	16 27 17.68	-24 25 53.5	15.70	900	2.88	3800 ⁺²⁰⁰ ₋₄₀₀	indet.	24.7	D
#4450	bdc	16 27 25.35	-24 25 37.5	17.71	1080	1.43	1400±100	3.0 ^{+1.7} _{-0.5}	15.6	C
SDSS 1254-0122	T2	12 54 53.90	-01 22 47.4	13.84	450	1.06	1500±100	5.0±0.5	0.0	C
2MASS 1503+2525	T5.5	15 03 19.61	+25 25 19.6	13.96	900	1.06	1100±100	5.0±0.5	0.7	S
NGC 4361 ^h	PN★	12 24 30.76	-18 47 05.4	14.02	450	1.29
Oph S1 ^h	A0	16 26 34.17	-24 23 28.3	6.32	6.1	1.74,1.80
HD 161743 ^h	A0	17 48 57.93	-38 07 07.5	7.57	6.1	3.09

Note. — Spectral types and K magnitudes for the two known T dwarfs are from Burgasser et al. (2003), Leggett et al. (2000), and Dahn et al. (2002). The last four columns of the table represent the results of model fitting, as described in the text.

^aDesignation “bdc” means that the object was a brown dwarf candidate

^bIntegration time

^cAir mass of observation

^dDesignation “indet.” means that the quantity was indeterminate from the model fits

^eUncertainty in A_V is ±2.5 mag for #4450, and ±1.0 mag in all other cases

^fBest fit model: N=NextGen, D=DUSTY, S=SETTL, C=COND

^gCorresponds to 16273288-2428116 in the 2MASS Point Source Catalog

^hUsed as calibrator